Iraqi Journal of Science, 2023, Vol. 64, No. 12, pp: 6620- 6637
DOI: 10.24996/ijs.2023.64.12.41

ISSN: 0067-2904

Investigation of the Baryonic Mass Tully–Fisher Relationship for Normal and Barred Spiral Galaxies

Al Najm M.N.[1*], Hasanain Hassan AL-Dahlaki[1] and Alkotbe Bashar A.[2]
[1] *Department of Astronomy and Space, College of Science, University of Baghdad, Baghdad, Iraq.*
[2]*Department of Physics, College of Science, University of Karbala, Karbala, Iraq.*

Received: 9/3/2022 Accepted: 13/5/2023 Published: 30/12/2023

Abstract

In this study, the stellar mass M*(L_B) and the atomic gas mass M_{HI} (L_B) were utilized to evaluate the baryonic mass Tully–Fisher (M_b) of disc system spiral galaxies (for normal spiral and barred spirals) and to obtain an empirical relation between masses M_b, M_{HI}, M* and optical luminosity at blue range L_B. The data for the studied sample was collected from literature papers for unbarred (normal) and barred-type morphological spiral galaxies. Therefore, in this work, the sample of data was chosen to analyze the baryonic mass Tully–Fisher relationship for normal and barred spiral galaxies. Statistical analysis of the connections was used between the stellar mass M*, the baryonic mass of disk spiral systems (M_b), and the M_{HI} for cold gas content. This study shows that there are certain relations and strong interconnections between the maximum and minimum baryonic mass ranges between M_{bmax} (L_B) ≈ $1.4x10^{12}$ $M_\odot$ and M_{bmin} (L_B) ≈ $2x10^9$ $M_\odot$ for barred, while M_{bmax} (L_B) ≈ $6x10^{11}$ $M_\odot$ and M_{bmin} (L_B) ≈ $5x10^9$ $M_\odot$ for unbarred spirals. Also, there are strong significant correlations between (Log M* - Log L_B and Log M_b - Log L_B). Finally, the analysis of the result demonstrates a strong partial coefficient correlation (R ~ 0.9) between the logarithmic scales relationships of baryonic mass (M_b) and the neutral cold gas mass (M_{HI}) for barred and unbarred spirals with a slope equal to 1.

Keywords: Spiral Galaxies, Baryonic Mass, Stellar Disk, Neutral Hydrogen, Tully - Fisher.

استقصاء علاقة الكتلة الباريونية لتولي– فيشر للمجرات الحلزونية العادية والقضيبية

محمد ناجي ال نجم[1*], حسنين حسن الدهلكي[1], بشار علاء الكتبي[2]
[1] قسم الفلك والفضاء، كلية العلوم، جامعة بغداد، بغداد ، العراق
[2] قسم الفيزياء ، كلية العلوم ، جامعة كربلاء ، كربلاء ، العراق

الخلاصة

في هذه الدراسة ، تم استخدام الكتلة النجمية (L_B) M * وكتلة الغاز الذري MHI (L_B) لتقدير الكتلة الباريونية لتولي – فيشر (M_b) لنظام المجرات الحلزونية القرصي (للحلزونيات العادية والقضيبية) والحصول على علاقة تجريبية بين الكتل M_b و MHI و M * والضيائية البصرية عند النطاق الأزرق L_B . تم دراسة عينة من البيانات التي تم جمعها من الأوراق الأدبية للمجرات الحلزونية القضيبية وغير القضيبية (العادية). لذلك ، في هذا العمل ، اختيرت بيانات العينة لتحليل العلاقة بين الكتلة الباريونية لتولي – فيشر للمجرات الحلزونية العادية والقضيبية. استخدم تحليلًا إحصائيًا للارتباطات بين الكتلة النجمية M * ، والكتلة الباريونية للأنظمة القرصية الحلزونية (M_b) و لمحتوى الغاز البارد MHI. أظهرت هذه الدراسة أن هناك علاقات معينة وترابطًا

*Email: mohalnajm@uobaghdad.edu.iq

قويًا بين مدى الحد الأقصى والأدنى للكتلة الباريونية يتراوح بين M_{bmax} (L_B) $\approx 1.4x10^{12}$ $M_\odot$ و M_{bmin} (L_B) $\approx 2x10^9$ $M_\odot$ للحلزونية القضيبية ، بينما M_{bmax} (L_B) $\approx 6x10^{11}$ $M_\odot$ و M_{bmin} (L_B) $\approx 5x10^9$ $M_\odot$ للحلزونية غيرالقضيبية. كما توجد ارتباطات معنوية قوية بين (Log M^* – Log L_B and Log M_b – Log L_B). أخيرًا ، اظهرت نتائج التحليل عن وجود معامل ارتباط جزئي قوي ($R \sim 0.9$) بين علاقات المقاييس اللوغاريتمية للكتلة الباريونية (M_b) وكتلة الغاز الطبيعي البارد (MHI) للحلزونات القضيبية وغير القضيبية مع ميل يساوي الواحد.

1. Introduction

The spiral structure is a characteristic of the disc. The Hubble sequence can be interpreted as a sequence in which the bulge/disk ratio decreases going from the first to the last types of galaxies. The spirals can contain a bar. The difference between barred and non-barred spirals is that the central core is approximately spherical in the case of normal spirals and decidedly elongated to form a bar in the case of the others **[1]**. Spiral galaxies are divided into Sa, Sb, and Sc, and barred spirals SBa, SBd, and SBc. The letters: a, b, and c refer to the dimensions of the core and the screwing of the spiral arms, respectively. In particular, the dimensions of the core become smaller and the arms are less screwed when switching from a to c.

The types Sd and SBd were later added to the original Hubble classification. As for the increased detail with which spirals are observed today, it has been seen that many of them have small triaxle bars in their central regions, and this makes the distinction between S and SB less clear **[2]**.

Recent terrestrial and space-based observations have made it possible for us to investigate the physical characteristics of millions of galaxies in the observable universe and the high-redshift universe. The study of the stellar components of galaxies has been a huge focus of these analyses. They allowed us to understand when and where star creation took place during cosmic periods much better.

To fully comprehend the process of galaxy formation, we should also carefully observe the neutral atomic hydrogen or HI; in reality, it serves as the starting point for the birth of stars. Based on the conventional theory, protogalactic halos all began with the same cosmic amount of gas, or roughly “1/6” of the host halo mass, in the form of a heated atmosphere. Then, it is anticipated that a portion of these warm baryons will cool and condense into a component of the cold gaseous disk-like structure, resulting in the formation of stars **[3]**. In the spiral galaxies' arms and nucleus, the pace of star production has essentially stayed constant over time. It indicates that the galaxy's spiral arms and nucleus are either constantly receiving gas input or that the efficiency of star creation in these regions has improved over time **[4]**. The power input from Type II supernova SN's outbursts and stellar winds can then deplete this frigid, star-forming gas to a degree controlled by the proportion between the amount of energy insinuated and the depth of the host halo's potential well. Moreover, the former depends on the mass of the host halo, whereas the latter depends on the total mass of stars generated and, consequently, the galaxy's luminosity **[5]**. So, observable data on the HI mass composition of galaxies places limitations on ideas relating to galaxy formation. A good scenario must replicate the stellar mass function, luminosity function "LF", cold hydrogen gas HI mass function, and correlations between the HI and stellar-to-halo masses in addition to the measured stellar mass function and luminosity function **[6]**.

According to Tully, the relationship between a galaxy's brightness and rotational speed is known as the Tully-Fisher (TF) connection **[7]**. Frequently, it has been utilized to calculate extragalactic distances **[8]**. In the standard "classical" interpretation, luminosity serves as a

stand-in for star mass and depends on the total mass (visible/dark masses) and, in turn, on the rotation speed. The central surface brightness of galaxies has no bearing on this conventional TF relation's slope or zero point **[9]**. The slope does, yet, seem to become steeper for very low-mass dwarf galaxies **[10]**. Due to their rotational speed, low-mass dwarf galaxies are under - luminous, which causes them to deviate from the TF relation established by high-mass galaxies. One can recreate a single linear connection by substituting the luminosity (or star mass) with the mass of the baryonic disk, which contains the hydrogen gas mass M_{HI} **[11]**.

The baryonic Tully-Fisher (BTF) relation is the name given to this relationship, which has recently been the subject of extensive studies **[12]**. Theoretical predictions for galaxy formation and development are severely constrained by the baryonic Tully-Fisher relation **[13]**. The measured dispersion in the TF relation places upper bounds on the extent of dark matter halos, according to Franx & de Zeeuw **[14]**. The Franx & de Zeeuw predict that the potential ellipticity in the disk's plane will probably be between 0 and 0.06. The study in the literature paper [15] led to the conclusion that the Tully-Fisher relationship is affected by morphological type dependence, resulting in galaxies with morphologies resembling ScI galaxies and Seyfert galaxies more luminous at a given rotation speed than galaxies with morphologies belonging to other morphological categories.

This work also shows how Tully-Fisher relationships significantly enhance the distances to individual galaxies and the precise distances to galaxy clusters. Because of the observed BTF relation's smaller scatter **[16]**, lower-mass galaxies can likewise be subject to the same limitations. They investigated the BTF for many dwarf galaxies with clearly discernible HI rotation curves and discovered a linear BTF relation with negligible scatter. Studies have also been done on the BTF relation's low mass end **[17]**. They estimated line widths at the level of 20% (W_{20}). They discovered that the intense dwarf galaxies in their sample exhibit the same BTF relation as the high-mass galaxies, despite a higher scatter. They corrected them for enlarging due to the tumultuous motion of the HI. They most certainly used the (W_{20})profile, which is the cause of the increased scatter. A. H. Broeils noted that, compared to line width measurements, employing the maximum rotation velocity from a determined rotation curve significantly reduces spread [18]. This paper is organised as follows: we describe data collection for our sample in Section 2 and identify the parameter that results in an expected total of baryons in spiral galaxies. We examine the findings and discussion in Section 3. Eventually, we briefly outline some of the conclusions of this work in Section 4.

2. The collected sample of data and finding the parameters

2.1 Data Collection

In this paper, our sample was collected from literature papers on unbarred and barred-type morphological spiral galaxies **[19] [20] [21] [22] [23] [24] [25] [26] [27] [28]**. Redshift (z) of the sample gathered from the website NASA /IPAC Extragalactic Database "NED". Important parameters, including the blue-band absolute magnitude MB and the apparent blue-magnitude mBtc corrected for galactic extinction, were obtained from the website HyperLEDA (De Lyon "France" and the Special Astrophysical Observatory "Russia" for Extragalactic Database). Based on HyperLEDA websites, the absolute magnitude is calculated using the distance modulus from the redshift and the corrected magnitude m_{Btc} redshift-independent. Table 1 contains the data for each of the chosen barred and unbarred spiral galaxies. All parameters mentioned in Table (1) are described in order. Column (1) shows the names of the galaxies. Column (2) gives the types of morphology. Columns (3) and (4) as well as (5) list the redshift z, the total apparent blue-magnitude m_{Btc}, and the blue absolute magnitude MB for the barred and unbarred galaxies. Note: Morphological type, whereby the letters S refer to unbarred spirals identified utilize unbarred spiral type from the earlier to most recent stages of the Hubble

sequence (S0, Sa, Sb, Sc, Sd, Sm), and SB stands for barred spiral galaxies (SB0, SBa, SBb, SBc, SBd, SBm).

Table 1: Information about the Parameters Utilized in the Study and Collected from the Literature for Unbarred Spiral Galaxies [19-28] and from the NED and HyperLEDA websites

No.	Name galaxy	Type	z	m_{Btc}	M_B
1.	NGC 1068	Sb	0.00379	9.47	-20.64
2.	NGC 1353	Sb	0.00509	11.63	-20.5
3.	NGC 1365	Sb	0.00546	9.82	-21.36
4.	NGC 1672	Sb	0.00444	10.15	-20.8
5.	NGC 3673	Sb	0.00647	11.94	-19.59
6.	NGC 1808	Sa	0.00334	10.28	-20.17
7.	NGC 4594	Sa	0.00342	8.7	-20.97
8.	NGC 7213	Sa	0.00584	10.81	-21.05
9.	NGC 0160	Sa	0.01753	13.34	-21.1
10.	NGC 0257	Sc	0.01761	12.79	-21.63
11.	NGC 1070	Sb	0.01364	12.51	-21.32
12.	NGC 2805	Sc	0.00578	11.4	-20.85
13.	NGC 4470	Sc	0.00781	12.73	-18.85
14.	NGC 5656	Sb	0.01049	12.55	-21.2
15.	NGC 6155	Sc	0.00805	12.68	-19.74
16.	NGC 7625	Sa	0.00543	12.8	-19.22
17.	NGC 7653	Sb	0.0142	13.01	-20.99
18.	NGC 7716	Sb	0.00856	12.56	-20.28
19.	NGC 7782	Sb	0.01786	12.48	-21.99
20.	NGC 7819	Sc	0.01653	13.6	-20.73
21.	UGC 12224	Sc	0.0117	14.72	-18.84
22.	UGC 12816	Sc	0.01775	14.04	-20.4
23.	NGC 2648	Sa	0.00727	12.33	-20.05
24.	NGC 2878	Sa	0.02432	14.25	-20.88
25.	NGC 0015	Sa	0.02112	14.56	-20.28
26.	UGC 06163	Sa	0.02121	14.33	-20.54
27.	NGC 7025	Sa	0.01657	13.42	-20.95
28.	NGC 6081	S0	0.01705	14.06	-20.38
29.	NGC 0774	S0	0.01533	13.95	-20.17
30.	NGC 201	Sc	0.01458	13.35	-20.64
31.	NGC 578	Sc	0.00543	11.11	-20.16
32.	NGC 685	Sc	0.00455	11.58	-19.45
33.	NGC 783	Sc	0.01731	11.98	-21.96
34.	NGC 800	Sc	0.01977	14.02	-20.65
35.	NGC 895	Sc	0.00763	11.87	-20.84
36.	NGC 977	Sa	0.01527	13.8	-20.26
37.	NGC 1187	Sc	0.00464	11.03	-20.36

38.	NGC 1385	Sc	0.005	11.01	-19.2
39.	NGC 1512	Sa	0.00299	10.74	-19.66
40.	NGC 3359	Sc	0.00338	10.75	-20.87
41.	NGC 3726	Sc	0.00288	10.27	-20.37
42.	NGC 4136	Sc	0.00202	11.76	-18.53
43.	NGC 4156	Sb	0.02262	13.71	-21.32
44.	NGC 4210	Sb	0.00904	13.06	-20.13
45.	NGC 4487	Sc	0.00346	11.23	-19.17
46.	NGC 4701	Sc	0.00241	12.43	-18.68
47.	NGC 4734	Sc	0.02504	13.9	-21.31
48.	NGC 4902	Sb	0.00892	11.5	-21.41
49.	NGC 4947	Sb	0.00804	12.03	-20.19
50.	NGC 5227	Sb	0.01745	13.59	-20.84
51.	NGC 5327	Sb	0.01455	13.22	-20.83
52.	NGC 5334	Sc	0.00462	12.56	-19.13
53.	NGC 5345	Sa	0.02419	13.28	-21.86
54.	NGC 5494	Sc	0.00869	12.91	-20.08
55.	NGC 5643	Sc	0.004	9.95	-21.08
56.	NGC 5653	Sb	0.0119	12.69	-20.85
57.	NGC 5850	Sb	0.00849	11.4	-21.57
58.	NGC 5905	Sb	0.01131	13.06	-20.57
59.	NGC 6001	Sc	0.03327	13.99	-21.88
60.	NGC 6008	Sb	0.01621	13.67	-20.69
61.	NGC 6035	Sc	0.01587	13.73	-20.57
62.	NGC 6221	Sc	0.00498	9.69	-20.64
63.	NGC 6267	Sc	0.00994	13.4	-19.96
64.	NGC 6484	Sb	0.0104	12.6	-20.89
65.	NGC 6753	Sb	0.01057	11.5	-21.72
66.	NGC 6770	Sb	0.01281	12.24	-21.4
67.	NGC 6782	Sa	0.01308	12.19	-21.49
68.	NGC 6941	Sb	0.02074	13.61	-21.2
69.	NGC 6943	Sc	0.01039	11.45	-20.91
70.	NGC 6949	Sc	0.00922	13.06	-19.67
71.	NGC 6984	Sc	0.01558	12.66	-21.42
72.	NGC 7070	Sc	0.00792	12.55	-20.04
73.	NGC 7102	Sb	0.01614	13.48	-20.8
74.	NGC 7252	S0	0.01598	12.59	-21.56
75.	NGC 7323	Sb	0.01868	13.62	-20.99
76.	NGC 7418	Sc	0.00484	11.41	-19.74
77.	NGC 7424	Sc	0.00313	10.51	-19.78
78.	NGC 7678	Sc	0.01164	12.05	-21.21
79.	NGC 7713A	Sc	0.01001	12.88	-20.19
80.	NGC 7714	Sb	0.00933	12.52	-20.51
81.	IC 4	Sc	0.01669	13.61	-20.72

82.	IC 167	Sc	0.00981	12.9	-19.38
83.	IC 221	Sc	0.01697	13.14	-21.22
84.	IC 370	Sc	0.03243	14.39	-21.33
85.	IC 498	Sb	0.03383	14.27	-21.57
86.	IC 503	Sa	0.01376	13.81	-20.04
87.	IC 539	Sc	0.02352	13.91	-21.12
88.	IC 577	Sc	0.03003	14.35	-21.24
89.	IC 616	Sc	0.01926	14.2	-20.44
90.	IC 1132	Sc	0.0151	14.02	-20.17
91.	IC 1236	Sc	0.02009	13.79	-21.01
92.	IC 1301	Sc	0.01324	14.1	-19.88
93.	IC 1525	Sb	0.01675	12.44	-21.95
94.	IC 1607	Sc	0.01813	14.07	-20.4
95.	IC 1666	Sc	0.01628	14.03	-20.27
96.	IC 1734	Sc	0.01665	13.29	-20.88
97.	IC 1764	Sb	0.0169	13.69	-20.66
98.	IC 1953	Sc	0.00623	11.76	-20.16
99.	IC 2522	Sc	0.01007	12.39	-20.35
100.	IC 2537	Sc	0.00932	12.11	-20.65
101.	IC 2580	Sc	0.01047	12.93	-20.26
102.	IC 3062	Sc	0.02626	14.27	-21.05
103.	IC 3115	Sc	0.00245	13.3	-18.64
104.	IC 3253	Sc	0.00902	11.63	-20.64
105.	IC 3267	Sc	0.00413	13.99	-18.87
106.	IC 3827	Sc	0.01433	13.58	-20.39
107.	IC 4229	Sb	0.02319	13.99	-21.07
108.	IC 4248	Sc	0.01369	13.26	-20.58
109.	IC 4341	Sc	0.00782	14.63	-18.24
110.	IC 4359	Sc	0.01381	13.16	-20.66
111.	IC 4366	Sc	0.01541	12.75	-21.34
112.	IC 4441	Sc	0.00654	13.65	-20.36
113.	IC 4479	Sc	0.04537	14.64	-21.9
114.	IC 4567	Sc	0.01913	13.15	-21.42
115.	IC 4633	Sc	0.0098	12.15	-20.44
116.	IC 4641	Sc	0.01779	13.7	-20.65
117.	IC 4646	Sc	0.01058	11.89	-21.33
118.	IC 4661	Sc	0.01611	13	-21.13
119.	IC 4688	Sc	0.0201	13.85	-20.94
120.	IC 4729	Sc	0.01481	12.44	-21.51
121.	NGC 1642	Sc	0.01542	12.85	-21.22
122.	NGC 2599	Sa	0.01585	12.91	-21.3
123.	NGC 4138	S0	0.00292	12.22	-18.48
124.	NGC 5297	Sc	0.00804	11.33	-21.26
125.	UGC 10692	Sb	0.03107	14.02	-21.71

Table 2: Information about the Parameters Utilized in the Study and Collected from the Literature for Unbarred Spiral Galaxies [19-28] and from the NED and HyperLEDA website

No.	Name galaxy	Type	z	m_{Btc}	M_B
1.	IC 4566	SBb	0.01857	13.7	-20.96
2.	NGC 0036	SBb	0.02011	13.75	-20.83
3.	NGC 0165	SBb	0.01964	13.5	-21.13
4.	NGC 0171	SBb	0.01304	12.58	-21.1
5.	NGC 0237	SBc	0.01391	13.28	-20.61
6.	NGC 0570	SBb	0.01843	13.37	-21.12
7.	NGC 0768	SBc	0.02328	13.37	-21.65
8.	NGC 0776	SBb	0.01641	12.94	-21.34
9.	NGC 2604	SBd	0.00694	13.38	-19.09
10.	NGC 2730	SBc	0.01276	13.32	-20.41
11.	NGC 3057	SBd	0.00508	13.12	-18.46
12.	NGC 3381	SBd	0.00543	12.72	-19.34
13.	NGC 3687	SBb	0.00835	12.18	-20.76
14.	NGC 5378	SBb	0.00996	13.43	-19.92
15.	NGC 5406	SBb	0.01797	12.8	-21.77
16.	NGC 5957	SBb	0.00605	13.33	-19.01
17.	NGC 6941	SBb	0.02074	13.61	-21.2
18.	UGC 01918	SBb	0.01696	13.66	-20.69
19.	UGC 03253	SBb	0.01375	12.74	-21.27
20.	UGC 04195	SBb	0.01626	13.83	-20.35
21.	UGC 04308	SBc	0.01189	13.26	-20.31
22.	UGC 05108	SBb	0.02714	14.16	-21.23
23.	UGC 08781	SBb	0.02525	13.78	-21.49
24.	NGC 4260	SBa	0.00592	12.06	-20.74
25.	NGC 4643	SBa	0.00445	11.07	-20.51
26.	NGC 7563	SBa	0.01433	13.4	-20.62
27.	UGC 3685	SBb	0.00599	12.41	-19.88
28.	NGC 2487	SBc	0.0161	13	-21.25
29.	NGC 2523	SBb	0.01158	12.18	-21.06
30.	NGC 2543	SBb	0.00824	12.28	-20.24
31.	NGC 2712	SBb	0.00607	12.29	-20.14
32.	NGC 3346	SBc	0.00425	12.31	-19.08
33.	NGC 3367	SBc	0.01013	11.86	-21.42
34.	NGC 3485	SBb	0.00478	12.59	-19.11
35.	NGC 3507	SBb	0.00327	11.85	-19.1
36.	NGC 3729	SBa	0.00354	11.51	-20.07
37.	NGC 3811	SBc	0.01029	12.62	-20.68
38.	NGC 4123	SBc	0.00443	11.63	-19.89
39.	NGC 4779	SBb	0.00944	12.71	-20.34
40.	NGC 4999	SBb	0.01879	12.75	-21.85

41.	NGC 5350	SBb	0.00775	11.89	-20.45
42.	NGC 5375	SBa	0.00792	12.52	-20.35
43.	NGC 5698	SBb	0.01211	13.41	-20.61
44.	NGC 5970	SBc	0.00653	11.53	-20.73
45.	NGC 55	SBm	0.00044	6.54	-20.08
46.	NGC 3044	SBc	0.0043	11.06	-20.57
47.	NGC 3079	SBc	0.00369	9.97	-21.19
48.	NGC 4565	SBc	0.00428	8.97	-21.44
49.	NGC 4631	SBc	0.00203	7.99	-21.35
50.	NGC 5775	SBc	0.00559	10.98	-20.51
51.	NGC 7462	SBc	0.00355	11.06	-18.86
52.	NGC 5112	SBc	0.00325	12.2	-18.98
53.	NGC 5156	SBb	0.00997	11.79	-21.28
54.	NGC 5351	SBb	0.01204	12.57	-21.18
55.	NGC 5618	SBc	0.02386	13.4	-21.72
56.	NGC 5754	SBb	0.01469	13.8	-20.35
57.	NGC 6923	SBb	0.00943	11.9	-20.7
58.	NGC 7171	SBb	0.00907	12.43	-20.77
59.	NGC 7412	SBb	0.0057	11.51	-18.4
60.	IC 527	SBc	0.02291	14.45	-20.58
61.	IC 651	SBd	0.015	12.9	-21.15
62.	IC 1142	SBc	0.04665	14.5	-22.1
63.	IC 1562	SBc	0.01256	13.46	-20.1
64.	IC 2473	Sbc	0.02692	14.29	-21.09
65.	IC 2604	SBm	0.00545	14.6	-17.47
66.	IC 2947	SBm	0.04237	14.13	-22.25
67.	IC 3376	SBa	0.02378	13.97	-21.17
68.	IC 3407	SBb	0.02337	14.06	-21.03
69.	IC 4219	SBb	0.01218	13.18	-20.41
70.	IC 4237	SBb	0.00888	12.53	-19.83
71.	IC 4585	SBb	0.01213	12.05	-21.46
72.	IC 4836	SBc	0.01563	12.82	-21.23
73.	IC 4839	Sbc	0.00906	12.77	-20.1
74.	IC 4852	SBc	0.01473	12.84	-21.11
75.	IC 5005	SBc	0.01038	13.03	-20.22
76.	IC 5092	SBc	0.01083	12.76	-20.46
77.	IC 5261	SBc	0.0108	13.62	-19.68
78.	NGC 2273	SBa	0.00614	12.1	-20.29
79.	NGC 2748	SBa	0.00492	11.69	-19.73
80.	NGC 3393	SBa	0.01251	12.6	-21.01
81.	NGC 4945	SBc	0.00188	7.21	-20.49
82.	NGC 5495	SBc	0.02247	13.1	-21.85
83.	NGC 6926	SBb	0.02001	11.62	-23.1
84.	ESO 565-11	SB0	0.01575	13.31	-20.83

85.	NGC 1326	SB0	0.00454	11.3	-19.74
86.	NGC 1512	SBa	0.00299	10.74	-19.66
87.	NGC 1672	SBb	0.00444	10.15	-20.8
88.	NGC 1285	SBb	0.01751	12.92	-21.43
89.	NGC 1483	SBb	0.00383	13	-17.51
90.	NGC 3464	SBc	0.01247	12.49	-21.12
91.	NGC 3905	SBc	0.01923	12.92	-22.11
92.	NGC 5339	SBa	0.00914	12.54	-20.5
93.	NGC 6754	SBb	0.01086	12.16	-20.76

2.2. Finding the Parameters

1-The ratio of an object's actual transverse size to its angular size is known as the angular diameter distance (D_A) in megaparsecs Mpc. The transverse comoving distance (D_M) is directly proportional to the angular diameter distance [29] [30]:

$$D_A = \frac{D_M}{1+z} \quad (1)$$

The comoving distance is the separation in the sky caused by an angle between two objects with the same redshift as well as distance, described in the following equation:

$$D_M = \frac{c}{H_o} \frac{2[2-\Omega_M(1-z)-(2-\Omega_M)\sqrt{1+\Omega_M z}}{\Omega_M^2(1+z)} \quad (2)$$

Where c is the speed of light, H_o stands for the Hubble constant, and Ω_M is the current density parameter for the baryonic matter. In this work, we have adopted the quantities $\Omega_M = 0.308$, $H_o = 67.8$ *km/sec/Mpc* [31] [32].

The link between bolometric energy flux F and bolometric luminosity L determines luminosity distance D_L that is integrated across all frequencies [33]:

$$D_L = \sqrt{\frac{L}{4\pi F}} \quad (3)$$

It indicates that this is influenced by the angular diameter distance and the transverse comoving distance. Therefore, the luminosity distance was given by [29] [33]:

$$D_L = (1+z)^2 D_A = (1+z) D_M = \frac{c}{H_o} \frac{2[2-\Omega_M(1-z)-(2-\Omega_M)\sqrt{1+\Omega_M z}}{\Omega_M^2} \quad (4)$$

2-The luminosity of the galaxies in the blue-optical band (λ=4400A^0) in unit blue solar luminosity ($L_{B,\odot}$) using an absolute magnitude of the sun in the blue band $M_{B,\odot} = +5.48^m$ is computed by the method [34]:

$$M_B - M_{B,\odot} = -2.5 \log \frac{L_B}{L_{B,\odot}} \quad (5)$$

So, Eq. (5) can be re-written as:

$$L_B(L_{B,\odot}) = 10^{-0.4(M_B - 5.48)} \quad (6)$$

3- According to galaxy luminosity distance in unit *Mpc*, and total apparent blue magnitude adjusted for galactic extinction (m_{Btc}), the blue luminosity (L_B), expressed in solar units ($L_\odot$) [31] [35]:

$$L_B(L_\odot) = 10^{(12.192 - m_{Btc})/2.5} \; D_L^2 \quad (7)$$

4- Cold neutral gas content MHI at frequency $v=1.49$ *GHz*, and the total atomic gas (*HI*) flux intensity, *F21*, determined from the 21-cm line profile in absorption and emission, $m_{21} = -2.5 \log F_{21} + 17.40$, can be used to calculate the cold neutral atomic hydrogen, MHI.

The amount of hydrogen gas each galaxy has concerning one unit of optical blue luminosity to calculate the total mass of the gas in galaxies throughout the universe. The hydrogen gas amount function MHI(L_B) can then be obtained from the blue luminosity function [36]. Since integral HI stretched to the blue-optical radius, therefore, in this work, the mass of the cold gas $MHI\ (L_B)$ is determined by the formula [37]:

$$M_{HI}(L_B) = 1.6 \times 10^6 \left(\frac{L_B}{10^6 L_\odot}\right)^{0.81} \left[1 - 0.18\left(\frac{L_B}{10^8 L_\odot}\right)^{-0.4}\right] M_\odot \quad (8)$$

Substituting Eq. (7) into Eq. (8) leads to:

$$M_{HI}(L_B) = 1.6 \times 10^6 \left(\frac{10^{(12.192-m_{Btc})/2.5} D_L^2}{10^6 L_\odot}\right)^{0.81} \left[1 - 0.18\left(\frac{10^{(12.192-m_{Btc})/2.5} D_L^2}{10^8 L_\odot}\right)^{-0.4}\right] M_\odot \quad (9)$$

5- The mass of the stellar disk M_* as a function of L_B of many barred and unbarred spiral galaxies can be calculated with the following expression [37]:

$$M_*(L_B) = 3.7 \times 10^{10} \times \left[\left(\frac{L_B}{L_{10}}\right)^{1.23} G(L_B) + 9.5 \times 10^{-2} \left(\frac{L_B}{L_{10}}\right)^{0.98}\right] \ in\ solar\ units\ M_\odot \quad (10)$$

The quantity G(L_B) is defined in the following equation:

$$G(L_B) = e^{\left[-0.87 \times (log\frac{L_B}{L_\odot} - 0.64)^2\right]}$$

Depending on the coefficient $L_{10}=10^{10}$ $L_{B,\odot}$ and $L_B\left(L_{B,\odot}\right) = 10^{-0.4(M_B - 5.48)}$, then we can write equation (10) by the formula:

$$M_*(L_B) = 3.7 \times 10^{10} \times \left[\left(\frac{10^{-0.4(M_B-5.48)}}{10^{10} L_{B,\odot}}\right)^{1.23} \times e^{\left[-0.87 \times (log\frac{L_B}{L_\odot} - 0.64)^2\right]} + 9.5 \times 10^{-2} \left(\frac{10^{-0.4(M_B-5.48)}}{L_{10}}\right)^{0.98}\right] M_\odot \quad (11)$$

6- The baryonic mass galactic structure is determined by its internal kinetics, proving its cosmological importance by demonstrating its universality and intrinsic independence from the way it is calculated. Both barred and unbarred spiral galaxies contain two other hydrogen components that resemble discs: (1) molecular hydrogen gas (H_2) and carbon monoxide gas (CO), which are present but are currently taken into account by M_* due to their diffusion as the exponential stellar disk, and (2) ionized gas hydrogen (HII), whose mass is challenging to calculate due to the strong edge of the HI/HII shift. The HII component was regarded in previous studies as anonymous baryon dark matter. In this study the term "baryonic mass Mb" refers to the combined stellar disk mass and neutral gas mass [37] [38]. $M_b = M_* + M_{gas}$ is the overall mass of the baryonic disk. With the usual correction for helium and metals, the mass in gas is calculated from the measured HI mass: $M_{gas} = 1.33 M_{HI}$. The Tully–Fisher baryonic mass of a system of spiral disk galaxies is given by the formula [37] [38]:

$$M_b = 1.33 M_{HI} + M_* \quad (12)$$

As mentioned above in Eqs. (9) (11) and Eq. (12) yields:

$$M_b = 1.33 \left[1.6 \times 10^6 \left(\frac{10^{(12.192-m_{Btc})/2.5} D_L^2}{10^6 L_\odot}\right)^{0.81} \left[1 - 0.18\left(\frac{10^{(12.192-m_{Btc})/2.5} D_L^2}{10^8 L_\odot}\right)^{-0.4}\right] + 3.7 \times 10^{10} \times \left[\left(\frac{10^{-0.4(M_B-5.48)}}{10^{10} L_{B,\odot}}\right)^{1.23} \times e^{\left[-0.87 \times (log\frac{L_B}{L_\odot} - 0.64)^2\right]} + 9.5 \times 10^{-2} \left(\frac{10^{-0.4(M_B-5.48)}}{L_{10}}\right)^{0.98}\right]\right] \quad (13)$$

3. Results and Discussion

In this section, the relationships between the content of atomic gas hydrogen (M_{HI}), stellar disc mass (M^*), blue luminosity at 440nm of disk spiral systems (L_B), and baryonic mass (M_b) are described for several barred N=93, and normal (or unbarred) N=125, and spiral galaxies sample. In this work, "unbarred" denotes that these galaxies are normal spirals. The focal component investigation is used in our statistical analysis of barred (*SB*) and unbarred (*S*) spiral galaxies. A scatter plot is used to graphically show the correlation between two variables. The best way to describe the linear relationship between the variables is to fit a regression line [39]. The statistical program was used to process and analyse the various relationships between the variables and determine whether there is difficulty in multiple regression between the behaviours of the two variables. Such a correlation is also shown in the form of scattered plots. The linear partial correlation coefficient R has values around (+1) and (-1).

The regression value of "1" shows that the two parameters are perfectly correlated. In particular, there was either no connection or a weak regression association between the two components when the measured value of the regression correlation (R) was at or close to zero. A positive sign "+" denotes a favourable regression relationship, whereas a negative sign "-" denotes a negative regression association [39].

Results comparisons of cold gas content, star disk mass, baryonic mass, and blue luminosity show that barred and unbarred spirals are affected differently. The results obtained from this study revealed that the maximum and minimum values of the barred and unbarred spirals of absolute magnitude are equivalent to $-17 \gtrsim M_B \gtrsim -23$ and $-18 \gtrsim M_B \gtrsim -22$, respectively. The outcomes of the statistical investigation showed that for barred spirals, the average value of L_B with a standard error "±" is equivalent to $2.87 \times 10^{10} \pm 1.096\ L_\odot$. In contrast, the mean value of L_B in unbarred galaxies is $2.95 \times 10^{10} \pm 1.08\ L_\odot$. These barred and unbarred spiral galaxies have the highest blue luminosity with a maximum and minimum value of approximately $10^{10}\ L_\odot > L_B > 10^{11} L_\odot$. Recent studies have confirmed the existence of many galaxies that appear unbarred at visible wavelengths. Nevertheless, normal spirals are typically 0.1 larger than barred galaxies in the blue-band optical luminosity. So, unbarred galaxies are slightly bluer than barred galaxies in all morphological categories. On the other hand, the value of the maximum and minimum baryonic mass ranges between $M_{bmax}(L_B) \approx 1.4 \times 10^{12} M_\odot$ and $M_{bmin}(L_B) \approx 2 \times 10^9\ M_\odot$ for barred, while $M_{bmax}(L_B) \approx 6 \times 10^{11}\ M_\odot$ and $M_{bmin}(L_B) \approx 5 \times 10^9\ M_\odot$ for unbarred spirals.

Barred and unbarred galaxies were analysed concerning logarithmic stellar disc system mass, baryonic mass, and logarithm blue luminosity. We fitted log M_b, Log M^*, and log L_B on multiple linear regression. The findings of the statistical analysis revealed quite potent significant correlations between (Log M^*-Log L_B, Log M_b - Log L_B), with a very sturdy partial correlation coefficient ($R \sim 0.9$) and a very high probability ($P \leq 10^{-7}$) for both barred and unbarred spirals. Figures (1 and 2) demonstrate that the slope is linear (Slope ≈ 1). The slope and scattering line of the M^*-L_B link is equivalent to those for the M_b -L_B relation since stellar disc mass is the predominant component. In fitting agreement with equations (10 and 13), we find that stellar and baryonic masses rise more sharply with increasing blue luminosity. The scatter diagram, which is calculated to represent the aggregated correlations, is a graph of input information for these worksheets that is very helpful. The scatter diagram will explicitly display the individual significances in representations of their variances from the corresponding group points.

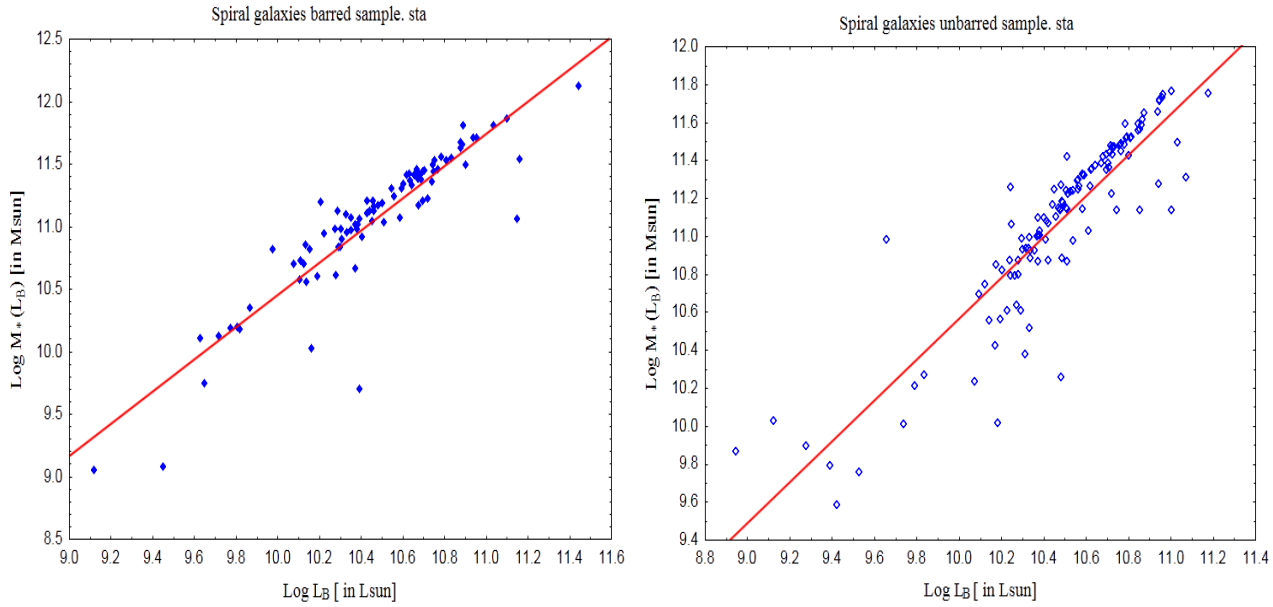

Figure 1: On the left: star mass $M_*(L_B)$ as a function of optical luminosity at blue range (L_B) for barred spiral galaxies. On the right: star mass $M_*(L_B)$ as a function of optical luminosity (L_B) for unbarred spiral galaxies.

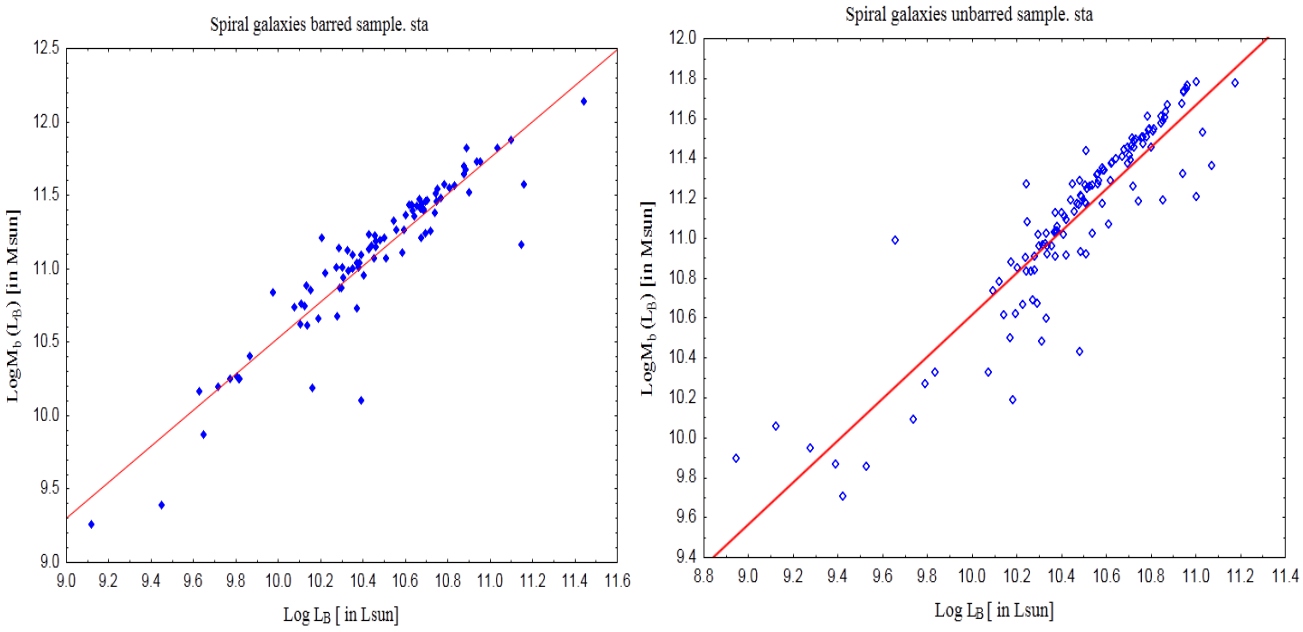

Figure 2: On the right: baryonic mass (M_b) as a function of optical luminosity at blue range (L_B) for barred spiral galaxies. On the left: baryonic mass (M_b) as a function of optical luminosity at blue range (L_B) for unbarred spiral galaxies.

Figure (3) shows the relation between the neutral hydrogen gas M_{HI} and luminosity blue-optical $L_{B,\odot}$ estimated in the blue region of the sun $M_{B,\odot} = +5.48^m$ of these galaxies, and demonstrates that there is a very significant link with a correlation coefficient ($R\sim 0.9$) for barred spiral galaxies, while a strong correlation ($R \sim 0.8$) is also noticed for the unbarred spiral galaxies, with a very steep probability ($P \leq 10^{-7}$) in the two cases. Pointing out that the slope of the line is linear and equal to one ($\text{Log } M_{HI} \alpha \text{ Log } L_{B,\odot}{}^{0.92\pm0.053}$ for unbarred and $\text{Log } M_{HI} \alpha \text{ Log}$

$L_{B,\odot}{}^{0.95\pm0.05}$ for barred) is significant in this point. The findings of our study's sample ($3x10^9 L_{B,\odot} \precsim L_B \precsim 10^{11} L_{B,\odot}$ for unbarred and $1.5x10^9\ L_{B,\odot} \precsim L_B \precsim 2.7x10^{11}\ L_{B,\odot}$ for barred) exhibit a powerful dominant link between the $M_{HI}(L_B)$ and L_B, with a mean value of logarithmic M_{HI} equal to (Log M_{HI}=9.792±0.029 $M_\odot$ for unbarred & Log M_{HI}=9.8±0.033 $M_\odot$ for barred galaxies. The reason for the different strengths of regression correlations between these spiral galaxies' types can be attributed to the fact that all types of spiral galaxies, according to the Hubble sequence, from the oldest stage to the newest, are atom-rich hydrogen gas HI, especially bars spiral. It becomes more difficult to determine whether the strength of a bar in a galaxy is adequate to rate a barred classification because there is a continuum of seeming bar strengths ranging from extremely small circular contortions to intrinsic characteristics. On the other hand, it is concluded that the speed dispersion caused by galactic spin across particular clouds typically expands the HI lines. The dispersal in barred galaxies' disc rotation curves is greater than in unbarred galaxies. As a result, the relationship between the cold gas content and blue luminosity of our sample galaxies (barred & unbarred) is various, intricate, and dependent on a variety of internal and external elements, including the surroundings, brightness, structure, and the origin of star formation activity, respectively.

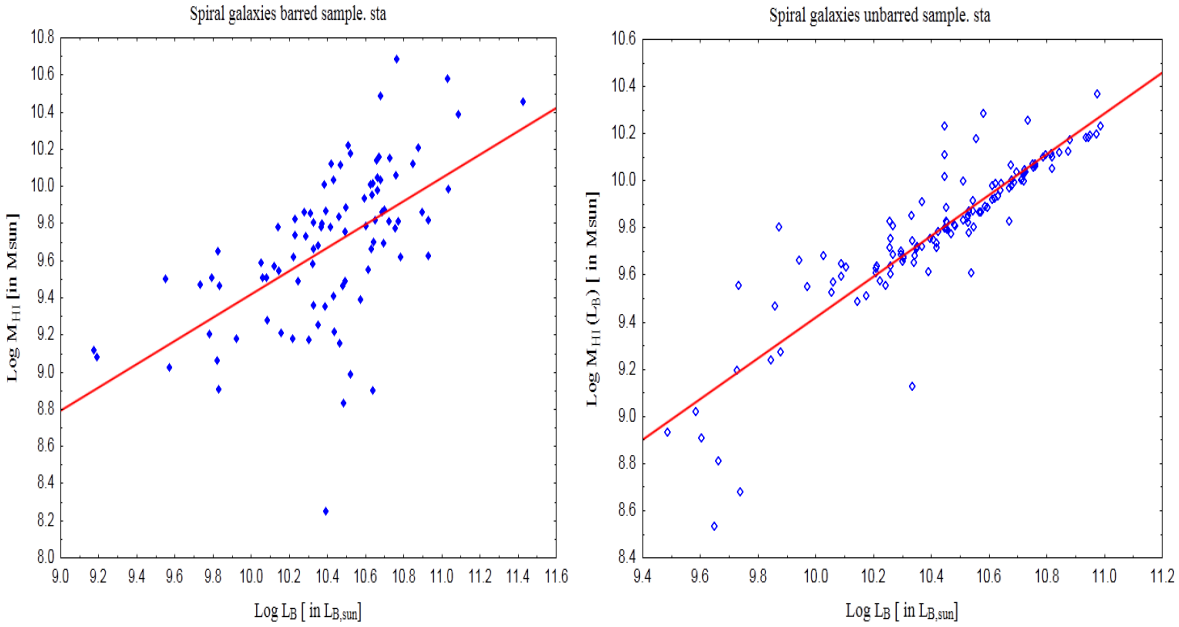

Figure-3 On the right: atomic gas mass (M_{HI}) as a function of optical luminosity at blue range (L_B) for barred spiral galaxies. On the left: atomic gas mass (M_{HI}) as a function of optical luminosity at blue range (L_B) for unbarred spiral galaxies.

In this paper, we also investigated the connections between the stellar mass (M_*), the baryonic mass of disk spiral systems (M_b), and the M_{HI} for cold gas content. The findings also revealed that there is a very strong partial correlation between the relationships of $LogM_*$ and $LogM_{HI}$, with a correlation coefficient (R) of 0.85 and a slope line of 0.78 for unbarred disc galaxies. Furthermore, the relationship between Log M_* and $LogM_{HI}$ has R-value of 0.87 with a regression value of (Log $M_* \alpha LogM_{HI}{}^{0.833\pm0.048}$) for barred disc galaxies, as well as a very strong probability ($P \leq 10^{-7}$) for the two cases. According to statistics, we infer that M_* and MHI have a close linear connection (slope ~ 1). The existence of a tight association between the logarithmic scales (M_b) and (M_{HI}) with a partial coefficient ($R \approx 0.9$) is also evident from our analysis. The stellar and baryonic masses for barred and unbarred spirals with slope ~1 are proportional to the atomic cold hydrogen masses Log M_*& Log $M_b \alpha LogM_{HI}$ (see Figures 4 & 5). The hydrogen-rich galaxies (both barred and unbarred) seem to be severe anomalies because they revolve too quickly for their blue brightness or star mass. These characteristics have been

viewed in the context of an essentially more basic link between the baryonic mass and the HI mass. The results of our analysis are consistent with those of instructive papers [37 and 38].

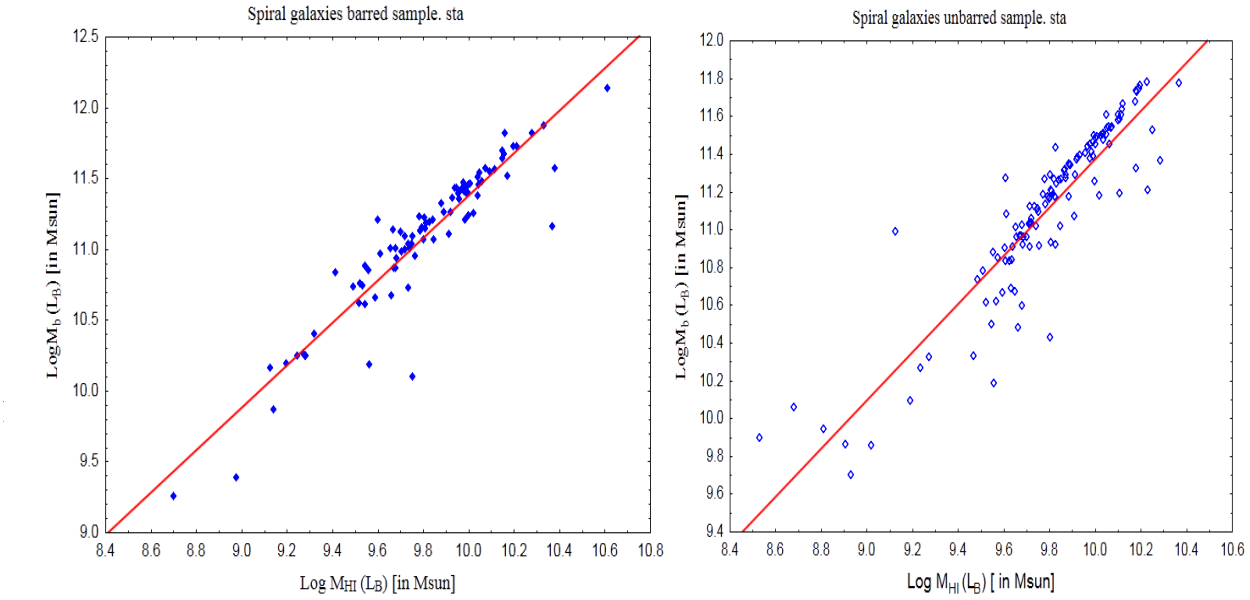

Figure 4: On the right: baryonic mass (M_b) as a function of atomic gas mass (M_{HI}) for barred spiral galaxies. On the left: baryonic mass (M_b) as a function of atomic gas mass (M_{HI}) for unbarred spiral galaxies.

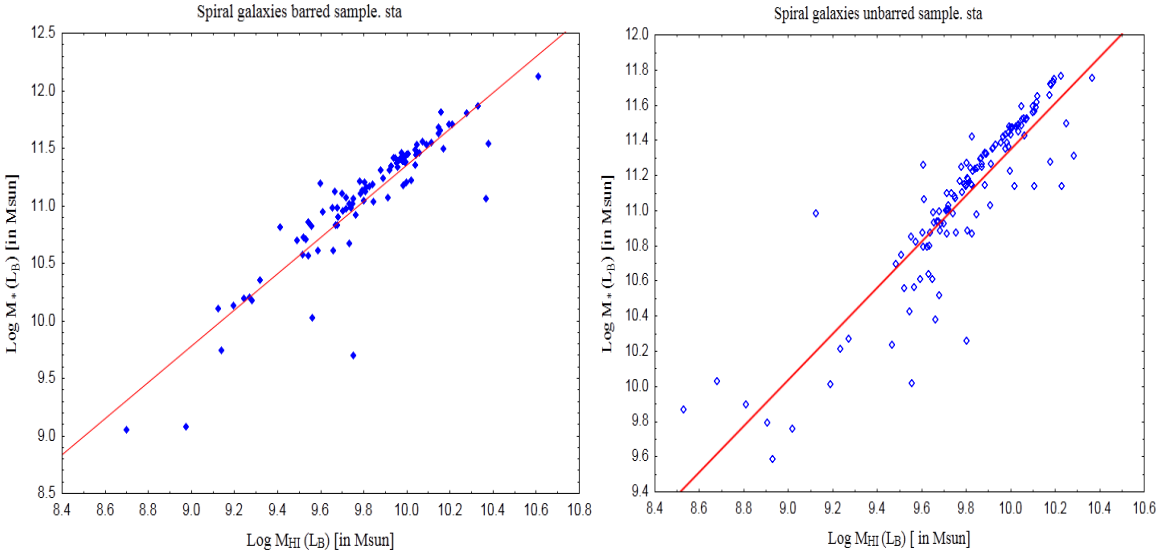

Figure 5: On the right: star mass (M_*) as a function of atomic gas mass (M_{HI}) for barred spiral galaxies. On the left: star mass (M_*) as a function of atomic gas mass (M_{HI}) for unbarred spiral galaxies.

Let us now explain how the baryonic mass relates to the ratio of star disc masses to atomic gas masses. There is a very steep relationship between Log (M^*/M_{HI}) and $LogM_b$ with a very robust partial correlation ($R \approx 0.81$) and a perfect significance probability ($P \leq 10^{-7}$) for barred, according to the linear regression equation of Figure (6a), which exhibits the following form: $Log\ M^*/M_{HI} \approx (0.84\pm0.07)\ LogM_b + (0.21\pm0.03)$ for barred spirals, here the value 0.84±0.07 is the finest approximation slope offering the smallest standard error, and 0.21±0.03 is the value

of the represented intercept with the y-axis with the standard error, whereas the formula for Figure (6b) is*: Log M*/M_{HI} ≈ (0.71±0.073) LogM_b+(0.6 ±0.04)*, which shows an intriguing link between these variables, with a very high probability ($P \leq 10^{-7}$) and a good correlation coefficient (R ≈ 0.66) between Log (MH*/M_{HI}) and Log M_b for unbarred galaxies. Further, we also revealed that the ratio M*/M_{HI} (of the stellar disc / extended cold gas) for our sample of unbarred spiral galaxies is roughly equal to 20. While the rate for our data of barred galaxies is M*/M_{HI} =17, indicating the mean value <M*/M_{HI}> for unbarred spirals is approximately equal to 1.2 <M*/M_{HI}> for barred spirals galaxies. The ratio of stellar disk mass to cold gas mass exhibits a tight positive association with the baryonic content in barred and unbarred spirals, with massive unbarred galaxies typically containing more gas and stars. Additionally, this implies that energy availability is a factor that distinguishes only galaxies that suffer starbursts from unbars, with the reason being the presence of a stellar disc that activates the operation of star generation in unbarred spiral galaxies.

Hydrogen gases HI, H_2, and HII are essential for forming stars, and they have a higher mass percentage in later spiral shapes. Peter Schneider demonstrated in 2015 [40] that about 0.04 for "Sa" early spirals, 0.08 for "Sb" intermediate spirals, 0.16 for "Sc-Sd" late spirals, and 0.25 for "Irr" irregular galaxies are characteristic values for the ratio (M_{HI}/M_b). In our current study, the ratio between the neutral hydrogen mass and the baryonic mass of the disk of spiral galaxies (M_{HI}/M_b) has been tested, and it was found to be approximately equal to ~ 0.05 for both unbarred and barred spirals. Our sample of galaxies for both types tend to be intermediate and late spirals (Sb-SBb, Sc-SBc, Sd-SBd, and Sm-SBm). Thus, it appears that late-type spirals have typically been more effective at converting their hydrogen gas into stars. Furthermore, for later Hubble categories, the proportion of molecular gas to the total gas mass is less.

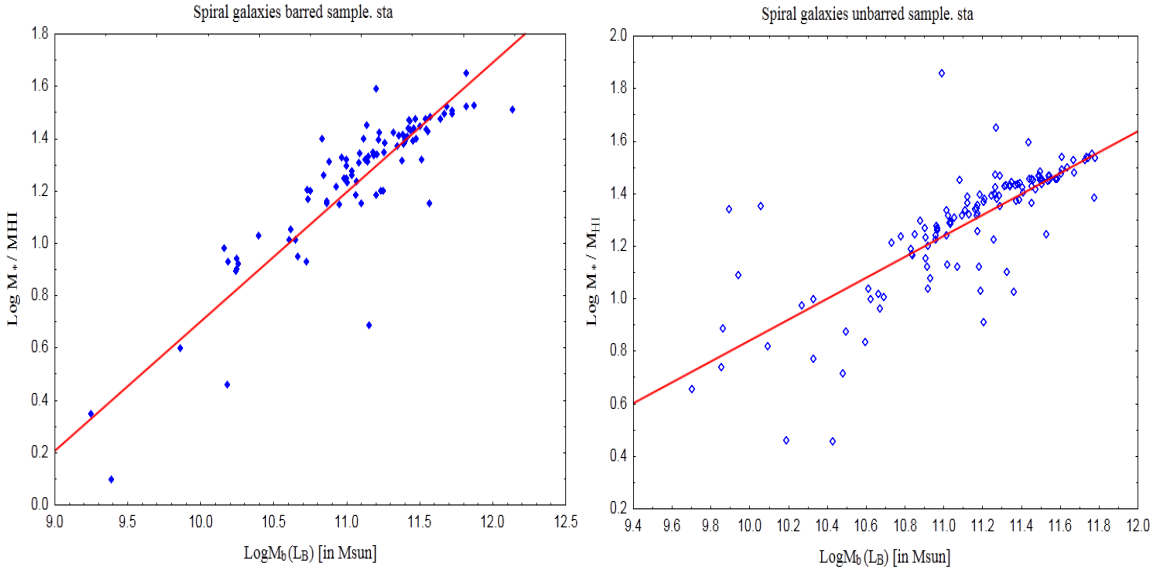

Figure 6: On the right: stellar mass (M_*) /atomic gas mass (M_{HI}) ratio as a function to baryonic mass (M_b) for barred spiral galaxies. On the left: stellar mass (M_*) /atomic gas mass (M_{HI}) ratio as a function to baryonic mass (M_b) for unbarred spiral galaxies.

5- Conclusion

This work investigates the baryonic mass Tully–Fisher relationship for normal and barred spiral galaxies. At the same time, our sample was collected from different literature papers for normal (unbarred) and barred-type morphological spiral galaxies. Our results can be terminated by focusing on the following main points:

1) The barred and unbarred spirals galaxies are affected differently. So the maximum and minimum values of the barred and unbarred spirals of absolute magnitude are equivalent to -17≳M_B ≳-23 and -18≳ M_B ≳-22, respectively.
2) Additionally, in this paper, we have shown that the values of the maximum and minimum baryonic masses range between M_{bmax} (L_B) ≈ 10^{12} $M_\odot$ and M_{bmin} (L_B) ≈ 10^9 $M_\odot$.
3) A considerable fraction of galaxies that appear unbarred at visible wavelengths are real, according to recent investigations. However, in the blue-band optical luminosity, normal spirals are generally 1/10 bigger than barred galaxies. Therefore, in all morphological classifications, unbarred galaxies are a little bit bluer than barred galaxies.
4) There are very strong significant correlations between (Log M* - Log L_B, Log M_b - Log L_B), with a very strong partial correlation coefficient (R ~ 0.9) and a very high probability (P ≤10^{-7}) for both barred and unbarred spirals. We believe that the slope and scattering line of the M*-L_B link is equivalent to the M_b -L_B relation since stellar disc mass. Furthermore, there is a significant link between the M_{HI}(L_B) and L_B, with a mean value of logarithmic M_{HI} equal to (Log M_{HI}=9.792±0.029 $M_\odot$ for unbarred and Log M_{HI}=9.8±0.033 $M_\odot$ for barred galaxies). The intense blue band emission intensity of these galaxies can be used to understand the material relevance of this essential relationship. The efficiency of stellar production, which is closely tied to blue luminescence, is also strongly influenced by stellar disk systems.
5) A strong relationship exists between the neutral hydrogen gas M_{HI} and luminosity blue-optical $L_{B,\odot}$ and there is a very significant link with a correlation coefficient (R~ 0.9) for barred spirals, while a strong correlation (R ~ 0.8) is also noticed for the unbarred spiral with a very steep probability (P ≤10^{-7}) in the two cases. As a consequence, the connection between the amount of cold hydrogen gas and the blue optical luminosity of our sample galaxies (barred & unbarred) is complex, variable, and dependent on a wide range of both internal and external factors, including the illumination, the formation, and the regions of star formation activity.
6) We furthermore discovered that while the ratio M^*/M_{HI} (of the stellar disk system/content cold hydrogen gas) is nearly equivalent to 20 for our sample of normal spiral galaxies, it is M^*/M_{HI} = 17 for our data of barred galaxies, denoting that the average value of $<M^*/M_{HI}>$ for normal (unbarred) is roughly equal to 1.2 $<M^*/M_{HI}>$ for the barred galaxies. The baryonic mass of barred and unbarred spirals galaxies is strongly significantly associated with the ratio of stellar disk mass to cold gas mass, with huge unbarred galaxies usually holding greater atomic hydrogen gas and stars.
7) Lastly, our study also shows that there is a strong correlation between the logarithmic scales (M_b) and (M_{HI}), with a partial coefficient correlation (R ~ 0.9). For barred and unbarred spirals, the baryonic and stellar masses are proportionate to the atomic cold hydrogen mass Log M_b & Log M* α Log M_{HI} with regression slope ~ 1. The barred and unbarred galaxies rich in cold hydrogen appear to be extreme oddities since their rotational velocities are proportional to their blue luminosity or stellar disk mass.

6- **Acknowledgments**

The authors are grateful to NASA /IPAC Extragalactic Database "NED" and HyperLEDA (De Lyon "France" and the Special Astrophysical Observatory "Russia" for Extragalactic Database). Many thanks to the University of Baghdad/ College of Science/ Department of Astronomy and Space for its support in finishing this paper. Also, the authors would like to thank the editors and the anonymous reviewers for their valuable comments and suggestions, which have helped immensely in improving the quality of the paper.

References

[1] J. Koeppen and N. Ariomoto, "The Hubble sequence of disk galaxies - A sequence of bulge-to-disk ratios," *Astronomy and Astrophysics*, vol. 240, no. 1, pp. 22- 35, 1990.

[2] T. H. Jarret, "Near-Infrared Galaxy Morphology Atlas", *The Publications of the Astronomical Society of the Pacific*, vol. 112 , no. 774, pp. 1008-1080, 2000.

[3] E. Komatsu, K. M. Smith, J. Dunkley, C. L. Bennett, B. Gold, G. Hinshaw, N. Jarosik, D. Larson, M. R. Nolta, L. Page, D. N. Spergel, M. Halpern, R. S. Hill, A. Kogut, M. Limon, S. S. Meyer, N. Odegard, G. S. Tucker, J. L. Weiland, E. Wollack, and E. L. Wright, "Seven-year Wilkinson Microwave Anisotropy Probe (WMAP) Observations: Cosmological Interpretation", *ApJS*, vol. 192, no. 18, 2011.

[4] H. Sinan Ali and Sundus A. Albakri, "BVR CCD Photometric observation analysis of spiral galaxy Ic 467", *Iraqi Journal of Physics*, vol. 12, no. 24, pp. 81-86, 2014.

[5] S.M . Fall and G. Efstathiou, "Formation and rotation of disc galaxies with haloes," *MNRAS*, vol. 193, no. 2, pp. 189-206, 1980.

[6] M. A. Zwaan, M. J. Meyer, L. Staveley-Smith and R. L. Webster, "The HIPASS catalogue: Ω_{HI} and environmental effects on the HI mass function of galaxies," *Monthly Notices of the Royal Astronomical Society*, vol. 359, no. 1, pp. L30-L34, 2005.

[7] R.B.Tully and J.R. Fisher, "A new method of determining distances to galaxies," *A.&A.*, vol. 54, no. 54, pp. 661-673, 1977.

[8] M.J.Pierce and R. B.Tully, "Distances to the Virgo and Ursa Major Clusters and a Determination of H_0," *ApJ*, vol. 330, pp. 579-595, 1988.

[9] M. A. Zwaan, J. M. van der Hulst, W. J. G. de Blok and S. S. McGaugh, "The Tully-Fisher relation for low surface brightness galaxies: implications for galaxy evolution", *MNRAS*, vol. 273, no. 1, pp. L35-L38, 1995.

[10] L. D.Matthews, W. van Driel and J. S.Gallagher, "An Exploration of The Tully-Fisher Relation For Extreme Late-Type Spiral Galaxies," *AJ*, vol. 116, no. 15, pp. 2196-2205, 1998.

[11] S. S.McGaugh, J. M. Schombert, G. D. Bothun and W. J. G. de Blok, "The Baryonic Tully-Fisher Relation", *ApJ*, vol. 533, pp. , L99-L102, 2000.

[12] E.F.Bell and R. S. de Jone, "Stellar Mass-to-Light Ratios and the Tully-Fisher Relation," *ApJ*, vol. 550, pp. 212-229, 2001.

[13] C. Trachternach, W. J. G. de Blok , S. S. McGaugh ,J. M. van der Hulst and R.-J. Dettmar, "The baryonic Tully-Fisher relation and its implication for dark matter halos", *Astronomy and Astrophysics*, vol. 505, pp. 577-587, 2009.

[14] M.Franx and T.de Zeeuw, "Elongated Disks and the Scatter in the Tully-Fisher Relation," *ApJ*, vol. 392, pp. L47-L50, 1992.

[15] G.David Russell, "Morphological Type Dependence in the Tully-Fisher Relationship," *ApJ*, vol. 607, no. 1, pp. 241-246, 2004.

[16] S. S. McGaugh, "The Baryonic Tully-Fisher Relation of Galaxies with Extended Rotation Curves and the Stellar Mass of Rotating Galaxies," *ApJ*, vol. 632, no. 2, pp. 859-871, 2005.

[17] M.Geha M. R. Blanton, M. Masjedi and A. A. West, "The Baryon Content of Extremely Low Mass Dwarf Galaxies," *ApJ*, vol. 653, pp. 240-254, 2006.

[18] A. H.Broeils, *Dark and visible matter in spiral galaxies*, Ph.D. Thesis,Univ. Groningen, 1992.

[19] I. Al-Baidhany, S.S. Chiad, W. A. Jabbar, N. F. Habubi and Kh.H. Abass, "Difference between Dynamical Masses and Stellar Masses of the Bulge in Spiral Galaxies", *NeuroQuantology*, vol. 18, no. 1, pp. 76-82, 2020.

[20] L. Sánchez-Menguiano, S. F. Sánchez, I. Pérez, R. García-Benito, B. Husemann, D. Mast, A. Mendoza, T. Ruiz-Lara, Y. Ascasibar, J. Bland-Hawthorn, O. Cavichia, A. I. Díaz, E. Florido, L. Galbany, R. M. Gónzalez Delgado, C. Kehrig, R. A. Marino and et al, "Shape of the oxygen abundance profiles in CALIFA face-on spiral galaxies," *Astronomy &Astrophysics*, vol. 587 , no. , A70, 2016.

[21] A. Fraser-McKelvie M. J. I. Brown, Kevin P., Tim D. and N. J. Bonne, "Multiple Mechanisms Quench Passive Spiral Galaxies," *Monthly Notices of the Royal Astronomical*, vol. 474, no. 1909, 2017.

[22] P. A. James and S. M.percival, "Star formation suppression and bar ages in nearby barred galaxies," *Monthly Notices of the Royal Astronomical Society,* vol. 474, no. 3, 2017.

[23] V. Heesen, M. Krause, R. Beck, B. Adebahr, D. J. Bomans, E. Carretti, M. Dumke, G. Heald, J. Irwin, B. S. Koribalski, D. D.Mulcahy, T. Westmeier and R. -J. Dettmar, "Radio haloes in nearby galaxies modelled with 1D cosmic-ray transport using SPINNA-KER," *Monthly Notices of the Royal Astronomical Society,* vol. 476, no. 158, 2018.

[24] M.A. Butenko and A.V.Khoperskov, "GALAXIES WITH "ROWS": A NEW CATALOG". *Astrophysical Bulletin,* vol. 72, no. 3, p. 232–250, 2017.

[25] L.Benjamin, A. W. Graham and E. Cameron, "Black Hole Mass Scaling Relations for Spiral Galaxies. II. M_{BH}- $M_{*,tot}$ and M_{BH}-$M_{*,Disk}$," *The Astrophysical Journal,* vol. 869, pp. 113-128, 2019.

[26] S. Aswathy and C. D. Ravikumar, "Co-evolution of Nuclear Rings, Bars and the Central Intensity Ratio of their Host Galaxies," *Research in Astronomy and Astrophysics,* vol. 20, no. 2, p. 15, 2019.

[27] L. Sánchez-Menguiano, S. F. Sánchez, I. Pérez, T. Ruiz-Lara, L. Galbany, J. P. Anderson, H. Kuncarayakti, "Arm-interarm gas abundance variations explored with MUSE: the role of spiral structure in the chemical enrichment of galaxies," *Monthly Notices of the Royal Astronomical Society,* vol. 492,pp. 4149–4163, 2020.

[28] D. I. Zobnina and A. V.Zasov, "Galaxies with Declining Rotation Curves", *Astronomy Reports,* vol. 97, no. 4, p. 267–283, 2020.

[29] D. W.Hogg, "Distance measures in cosmology," arXiv:astro-ph/9905116, 1999.

[30] H. Ahmed Abd Al-Lateef and H. Saad Mahdi, "The Dependence of The Gravitational Lensing Properties on The Lens And Source Redshifts," *Iraqi Journal of Science,* vol. 63, no. 2, pp. 866-876, 2022.

[31] K. A. Dua'a and M. N. Al Najm, "Investigation of the Characteristics of CO (1-0) Line Integrated Emission Intensity in Extragalactic Spiral," *Iraqi Journal of Science,* vol. 63, no. 3, pp. 1376-1394, 2022.

[32] H.K.Salwa and Y. E. Rashed," *Studying the Correlation between Supermassive Black Holes and Star Formation Rate for Samples of Seyfert Galaxies (Type 1 and 2)", Iraqi Journal of Physics* ,vol. 19, no. 4, pp. 52 -65, 2021.

[33] Y. E. Rashed, M. N. Al Najm and H. H. AlDahlaki, "Studying the Flux Density of Bright Active Galaxies at Different Spectral Bands," *Baghdad Science Journal,* vol. 16, no. 1, pp. 230-236, 2019.

[34] W.B. Carroll and A. Dale , " An Introduction to Modern Astrophysics," in *Second Edition, Pearson Education* , Addison-Wesley, Addison-Wesley, 2007, p. 973.

[35] H. H. AlDahlaki, "Calculation and comparison of certain physical properties of sample irregular galaxies with the Milky Way galaxy," *Karbala International Journal of Modern Science,* vol. 7, no. 4., pp. 374-385, 2021.

[36] J. I. Read and N.Trentham, "The baryonic mass function of galaxies," *Phil. Trans. R. Soc. A,* vol. 363, no. 1837, pp. 2693–2710, 2005.

[37] P.Salucci and M.persic, "The baryonic mass function of spiral galaxies: clues to galaxy formation," *Monthly Notices of the Royal Astronomical Society,* vol. 309, pp. 923-928, 1999.

[38] P.-F. Wu, "The scaling relationship between baryonic mass and stellar disc size in morphologically late-type galaxies," *Monthly Notices of the Royal Astronomical Society,* vol. 473, pp. 5468–5475, 2018.

[39] M. N. Al Najm, "Studying the Atomic and Molecular Hydrogen Mass (MHI, MH2) Properties of the Extragalactic Spectra," *Iraqi Journal of Science,* vol. 61, no. 5, pp. 1233-1243, 2020.

[40] Peter Schneider, "Extragalactic Astronomy and Cosmology an Introduction," New York, Springer Berlin Heidelberg, 2015, pp. 128-129.